ADVANCES IN ATMOSPHERIC SCIENCES, VOL. 31, SEPTEMBER 2014, 1051–1064

Relationships between Interannual and Intraseasonal Variations of the Asian–Western Pacific Summer Monsoon Hindcasted by BCC_CSM1.1(m)

LIU Xiangwen*[1], WU Tongwen[1], YANG Song[2], LI Qiaoping[1], CHENG Yanjie[1], LIANG Xiaoyun[1], FANG Yongjie[1], JIE Weihua[1], and NIE Suping[1]

[1]*National Climate Center, China Meteorological Administration, Beijing* 100081

[2]*Department of Atmospheric Sciences, Sun Yat-sen University, Guangzhou* 510275

(Received 9 October 2013; revised 6 January 2014; accepted 24 February 2014)

ABSTRACT

Using hindcasts of the Beijing Climate Center Climate System Model, the relationships between interannual variability (IAV) and intraseasonal variability (ISV) of the Asian–western Pacific summer monsoon are diagnosed. Predictions show reasonable skill with respect to some basic characteristics of the ISV and IAV of the western North Pacific summer monsoon (WNPSM) and the Indian summer monsoon (ISM). However, the links between the seasonally averaged ISV (SAISV) and seasonal mean of ISM are overestimated by the model. This deficiency may be partially attributable to the overestimated frequency of long breaks and underestimated frequency of long active spells of ISV in normal ISM years, although the model is capable of capturing the impact of ISV on the seasonal mean by its shift in the probability of phases.

Furthermore, the interannual relationships of seasonal mean, SAISV, and seasonally averaged long-wave variability (SALWV; i.e., the part with periods longer than the intraseasonal scale) of the WNPSM and ISM with SST and low-level circulation are examined. The observed seasonal mean, SAISV, and SALWV show similar correlation patterns with SST and atmospheric circulation, but with different details. However, the model presents these correlation distributions with unrealistically small differences among different scales, and it somewhat overestimates the teleconnection between monsoon and tropical central-eastern Pacific SST for the ISM, but underestimates it for the WNPSM, the latter of which is partially related to the too-rapid decrease in the impact of El Niño–Southern Oscillation with forecast time in the model.

Key words: interannual variability, intraseasonal variability, western North Pacific summer monsoon, Indian summer monsoon

Citation: Liu, X. W., and Coauthors, 2014: Relationships between interannual and intraseasonal variations of the Asian–western Pacific summer monsoon hindcasted by BCC_CSM1.1(m). *Adv. Atmos. Sci.*, **31**(5), 1051–1064, doi: 10.1007/s00376-014-3192-6.

1. Introduction

Because of its complex variability and significant economic and social impacts, prediction of monsoon has long been an important yet challenging task. As an important approach, dynamical prediction of monsoon has drawn much attention from both academic and operational communities. However, monsoon prediction with climate models suffers from many limitations, such as initial condition errors, imperfect model physics, incomplete forecast methods, among others. Therefore, monsoon prediction by state-of-the-art climate models still shows an inability to capture the climatological mean state (e.g., Lee et al., 2010; Li et al., 2012; Liu et al., 2013), spatial and temporal variability (e.g., Wang et al., 2008; Xue et al., 2010; Liu et al., 2014), and relationships between monsoon and other climate systems (e.g., Yang et al., 2008; Drbohlav and Krishnamurthy, 2010; Rajeevan et al., 2012). Thus, assessing the skills and diagnosing the deficiencies of dynamical monsoon prediction are important for improving monsoon prediction and model development.

As the strongest monsoon system in the world, the Asian–western Pacific summer monsoon is marked by significant multiscale variability. In particular, its interannual variability (IAV) and intraseasonal variability (ISV), known by their important impacts on many prominent climate and weather phenomena both inside and outside the monsoon region, have received much research interest (e.g., Wang et al., 2008; Xavier et al., 2008; Zhou et al., 2009; Yoo et al., 2010). Although with respective mechanisms and representations, the IAV and the ISV of monsoon are connected with each other and with other climate systems. The predictability of IAV

* Corresponding author: LIU Xiangwen
Email: xwliu@cma.gov.cn

of tropical monsoon is supposed to be originated from external forcing, such as SST, soil moisture, and snow cover (Charney and Shukla, 1981), while the ISV of monsoon often serves as an important but less predictable internal component (e.g., Goswami, 1998; Kang and Shukla, 2006; Suhas et al., 2012). However, it has also been hypothesized that the IAV of monsoon is determined by the shift in the probability density function of ISV toward either active or break phases, in which external boundary forcing may act as an essential modulating factor (Palmer, 1994; Ferranti et al., 1997; Sperber et al., 2000; Goswami and Ajaya Mohan, 2001). In this scenario, significant correlation between seasonal mean monsoon and ISV has been found for the South Asian summer monsoon (e.g., Lawrence and Webster, 2001; Waliser et al., 2004; Goswami et al., 2006; Qi et al., 2008; Fujinami et al., 2011), and the relationship between the ISV of summer monsoon and El Niño–Southern Oscillation (ENSO) has also been revealed (Teng and Wang, 2003; Kim et al., 2008; Qi et al., 2008). At present, it is still worth further exploring whether the ISV of monsoon is not entirely internal variability, but instead partially related to external components.

Also, as revealed by previous studies on the South Asian summer monsoon, the IAV of the seasonal mean consists of two independent parts: a large-scale seasonally persistent mean component, and an average of the ISV; and the predictability of the seasonal mean monsoon depends on the relative magnitudes of seasonal averages of the persistent component and the intraseasonal component (Krishnamurthy and Shukla, 2000, 2007, 2008). In this context, both observations and model simulations have proved the presence of a large-scale seasonally persistent structure that is attributable to external forcing and largely determines the IAV of seasonal mean monsoon, while the nature of ISV is less dependent on the IAV of monsoon (Achuthavarier and Krishnamurthy, 2010).

Although the connection and interaction between the IAV and ISV of monsoon is still a controversial issue, a reasonable reproduction of the relationship between IAV and ISV by climate models is indispensable for the skillful seasonal prediction of monsoon. Thus, in this study, we explore the relationships between the IAV and ISV of the Asian–western Pacific monsoon by comparisons between observations and model hindcasts, and between the western North Pacific summer monsoon (WNPSM) and the Indian summer monsoon (ISM). The following questions are addressed: are there significant relationships between the IAV and ISV of monsoon over this monsoon region? In what way and to what degree are the IAV and the ISV of monsoon connected with external forcing and background circulation? What are the differences in the above features between the WNPSM and ISM? How well can models reproduce the observed features?

In section 2, a brief overview of the model output, observational data, and analysis methods is provided. In sections 3–5, we analyze the predictions of basic monsoon features, the relationship between the ISV and IAV of monsoon, and the links with external forcing and atmospheric circulation, respectively. A summary and further discussion are presented in section 6.

2. Model, data and methods

The model used in this study is an updated version of the Beijing Climate Center (BCC) Climate System Model version 1.1 (BCC_CSM1.1; Wu et al., 2013) with a moderate atmospheric resolution [BCC_CSM1.1(m)]. The atmospheric component in BCC_CSM1.1(m) is the BCC Atmospheric General Model version 2 with a T106 horizontal resolution and 26 hybrid sigma/pressure layers in the vertical direction (Wu et al., 2010). The oceanic component is the Geophysical Fluid Dynamics Laboratory (GFDL) Modular Ocean Model version 4 with a tripolar grid in the horizontal direction and 40 levels in the vertical direction, and the sea ice component is the GFDL Sea Ice Simulator. The land model is the BCC Atmosphere and Vegetation Interaction Model version 1.0. The different components are coupled without any flux correction. The BCC_CSM1.1(m) and the BCC_CSM1.1 are two of the climate system models joining phase five of the Coupled Model Intercomparison Project (CMIP5). The reasonable performance of BCC_CSM1.1(m) in climate simulation and projection has been revealed by a fair number of studies listed on the website http://cmip.llnl.gov/cmip5/publications/model?exp=BCC-CSM1.1-m.

Some experiments aimed at boreal summer climate prediction are implemented using BCC_CSM1.1(m). The hindcasts are initiated from 1 March of each year from 1991 to 2010 and end with a 7-month integration. The atmospheric initial conditions are obtained from the winds, air temperature, and surface pressure of the National Centers for Environmental Prediction (NCEP) Reanalysis with four-times-daily output, and oceanic initial conditions are from the sea temperature of the NCEP Global Oceanic Data Assimilation System. These reanalysis data are used to initialize the model by a nudging strategy, which operates from late 1980 to the beginning of a certain retrospective forecast. Each hindcast includes 15 members, produced by a combination of lagged average forecasting on atmospheric and oceanic initials, and singular vector perturbing on initials of SST at the end of February in the hindcast year.

The observations used for model verification include various variables from the NCEP Reanalysis 2 (Kanamitsu et al., 2002), the Optimum Interpolation SST (Reynolds et al., 2002), and the daily mean outgoing longwave radiation (OLR; Liebmann and Smith, 1996) from the National Oceanic and Atmospheric Administration (NOAA), and the global monthly precipitation from the Climate Prediction Center Merged Analysis (Xie and Arkin, 1997).

The IAV of monsoon for a particular year refers to the difference of the June–July–August–September (JJAS) mean between the specific year and the climatology from 1991 to 2010, and the ISV is computed based on the daily mean series in that year with a subtraction of daily climatology and a subsequent filtering on the intraseasonal component, unless otherwise indicated. For the model output, the length of the daily anomaly series (daily means minus daily clima-

tologies) in each year is only 214 days (from 1 March to 30 September), which is unfavorable for using a Lanczos band-pass filter to extract the intraseasonal part. Thus, a Fourier harmonic analysis is performed on the time series and the leading three harmonics (period > 70 days) are first deducted as part of long-wave variability, followed by a 5-day running average on the residue to get the part of the ISV. Then, the results from June to September are chosen for the ISV in boreal summer. The same process is also used to extract observed ISV in each year from 1991 to 2010.

To focus on the variability of the WNPSM and ISM, two dynamical monsoon indices are used in our analyses. The WNPSM index (WNPSMI) and the ISM index (ISMI) are defined as the differences in area-averaged 850-hPa zonal wind between (5°–15°N, 100°–130°E) and (20°–30°N, 110°–140°E), and between (5°–15°N, 40°–80°E) and (20°–30°N, 70°–90°E), respectively (Wang et al., 2001). All the summer means, ISV and long-wave variability of each monsoon index are calculated with the methods mentioned above.

Additionally, we compute the direct correlations between predictions and observations using ensemble-averaged variables to better depict the performance of ensemble prediction. However, to objectively assess the model's ability, for comparisons of any feature between the predictions and observations, computations are first performed for individual members before averages are made.

3. Predictions of basic monsoon features

Figure 1 shows the climatologies of JJAS mean precipitation and 850-hPa winds for prediction, observations, and model biases. The model captures the major low-level features of the distribution of the Asian–western Pacific summer monsoon. It also captures the overall locations and magnitude of major rainfall and winds in many places. However, apparent systematic biases of the model are also found, which include a dry bias over most of the Bay of Bengal, a wet bias over the west coast of the Indo-China Peninsula, and a cyclonic wind bias over the northwestern Pacific associated with a wet bias over the central zone of the wind bias and dry biases over the South China Sea and the western edge of the Western Pacific Subtropical High (WPSH). With overall weaker magnitude, these biases also appear in the NCEP Climate Forecast System (e.g., Yang et al., 2008; Drbohlav and Krishnamurthy, 2010), and also some multi-model ensembles of the DEMETER and ENSEMBLES EU projects (e.g., Lee et al., 2010; Rajeevan et al., 2012), suggesting some common deficiencies of state-of-the-art climate models. Besides, significant convergence wind bias over the central tropical North Indian Ocean and divergence wind bias over the eastern tropical South Indian Ocean, along with wet and dry bias, respectively, exist in BCC_CSM1.1(m).

Despite the obvious systematic biases, a reasonable prediction skill of the model for monsoon variability is still expected. Figure 2 shows the temporal correlations between predictions and observations for interannual variations of JJAS mean 850-hPa zonal wind and precipitation. Significant skills for the forecast of low-level winds are mainly found over most of the tropical western North Pacific and East Asia, covering the majority of areas along the western edge of the WPSH. The model seems to perform better in predicting the WNPSM and East Asian summer monsoon than the South Asian summer monsoon, at least for atmospheric circulation. In contrast, except for some sparse regions near the equator, the prediction of rainfall shows little skill over most areas (Fig. 2b), consistent with previous results showing that the forecasting of precipitation often exhibits quicker error growth and shorter time in approaching the upper limit of predictability than circulation (e.g., Xie et al., 2012; Liu et al., 2014).

As important measures of monsoon variability, the intensities of the ISV and IAV of 850-hPa zonal wind, given by their respective standard deviations, are further explored (Fig. 3). The model reasonably reproduces the observed features of the distribution of ISV intensity with maximums over the extratropical North Pacific and areas from the Bay of Bengal to the Philippine Sea, as well as the distribution of IAV intensity with a magnitude center over the tropical western North Pacific induced by ENSO. Nevertheless, compared to observations, obviously stronger ISV intensity over most places and a more extensive and too-far-east center of magnitude are found. Meanwhile, the IAV shows a larger central intensity

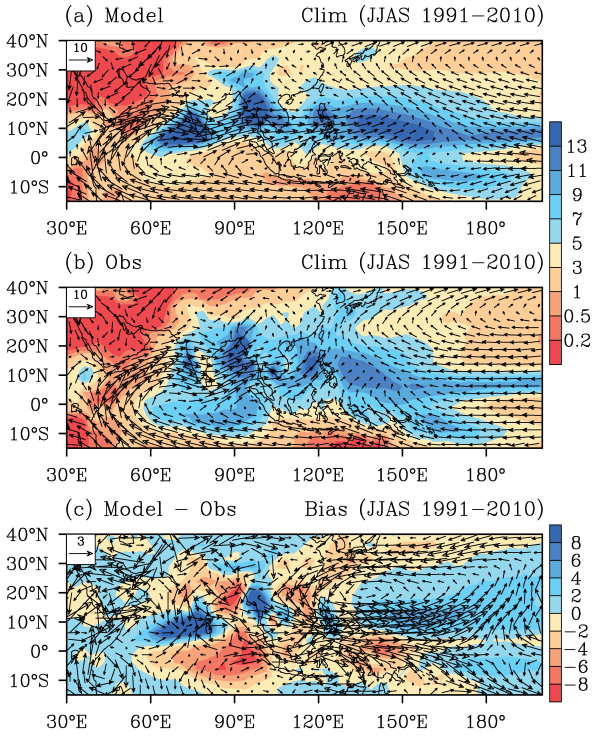

Fig. 1. 20-year means of precipitation (shading; units: mm d^{-1}) and 850-hPa winds (vectors; units: m s^{-1}) for (a) hindcasts, (b) observations, and (c) biases (predictions minus observations) averaged from June to September.

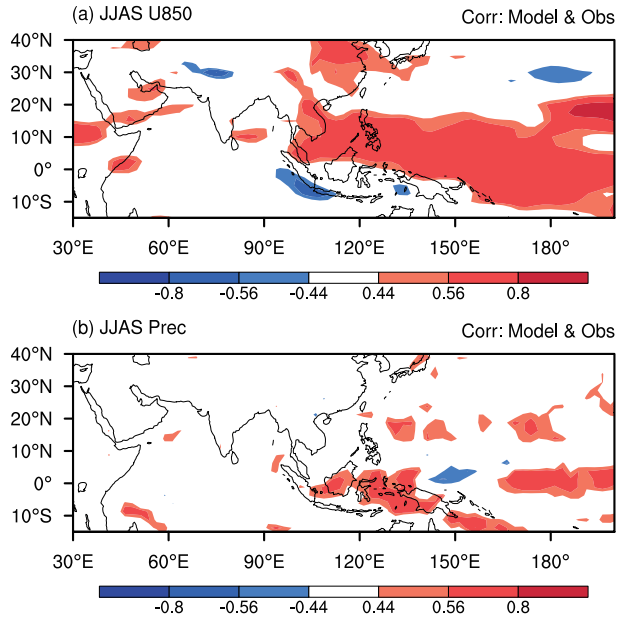

Fig. 2. Spatial distributions of temporal correlations between predictions and observations for summer-averaged (a) 850-hPa zonal wind and (b) precipitation from 1991 to 2010. The shading levels above 0.44 and 0.56 represent the statistical significance of correlation above the 95% and 99% confidence levels, respectively, and the same hereafter.

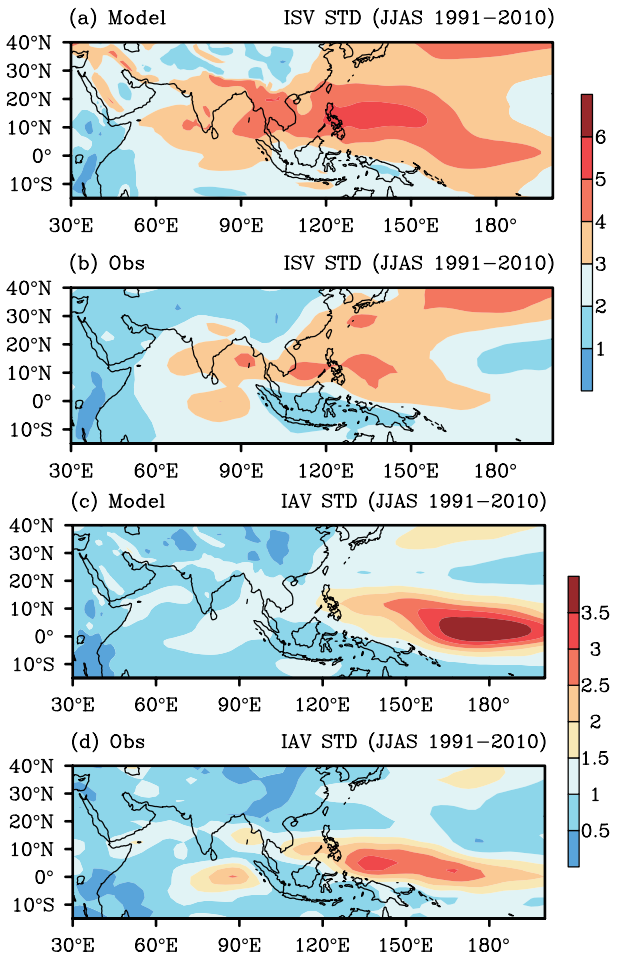

Fig. 3. Ensemble mean standard deviation (units: m s^{-1}) of intraseasonal variability in summer (top two rows) and interannual variability of summer mean (bottom two rows) for 850-hPa zonal wind from 1991 to 2010. Panels (a) and (c) are for the model, and (b) and (d) are for observations.

with a farther southeastward shift toward the dateline over the western Pacific in the model. In addition, because the ISV and IAV of monsoon may be governed by a common spatial mode of variability (Ferranti et al., 1997; Sperber et al., 2000; Goswami and Ajaya Mohan, 2001), the observed features given in Figs. 3b and d both show high intensity over the Bay of Bengal, the South China Sea, and the Philippine Sea, even though this is not well captured by the model for the false shifts of variability centers in Figs. 3a and c.

Next, we discuss some basic characteristics of ISV before exploring the relationships among different time scales. A similar-to-observed vertical structure (Figs. 4a and b) and northward propagation (Figs. 4e and f) are found for the ISV of the WNPSM in the model, albeit with a somewhat smaller range of the vorticity center and a faster propagation speed than in observations. For the ISV of the ISM, the model captures a slightly faster northward propagation (Figs. 4g and h) and a more northward center of vertical vorticity (Figs. 4c and d) compared to observations. Furthermore, the broadband spectrum of ISV and its resulting aperiodicity is one of the important characteristics in generating a non-trivial seasonal mean ISV anomaly, which partially acts as a bridge to connect the ISV and IAV of monsoon (Goswami and Xavier, 2005; Goswami et al., 2006). Thus, the spectral features of the ISV of the WNPSM and ISM are specifically examined in Fig. 5. Narrower-than-observed spectral bands are captured by the model for both the WNPSM and ISM. In particular, the predicted ISV does not show a significant period of near 50 days, which is the spectral peak found in observations. Besides, similar results can be derived by power spectral analyses for regionally averaged OLR over the WNPSM region (10°–25°N, 110°–140°E) and the ISM region (7.5°–22.5°N, 60°–90°E) (figures not shown). This feature is unfavorable for the seasonally accumulated quantity of ISV anomaly to contribute to the seasonal mean in the model since a narrow band may be periodic and its accumulation should show little residue in the whole season.

4. Relationship between the ISV and IAV of monsoon

In this section, the relationship between the ISV and IAV of the Asian–western Pacific summer monsoon is explored with a focus on the intensity, seasonally averaged anomaly, frequency of occurrence of positive (negative) phase, and frequency of consecutive break or active spells of ISV.

Figures 6a and b show the interannual correlations between the intensity of ISV and the summer mean for 850-hPa zonal wind in the model and observations. The intensity of ISV in boreal summer shows a significant positive correlation

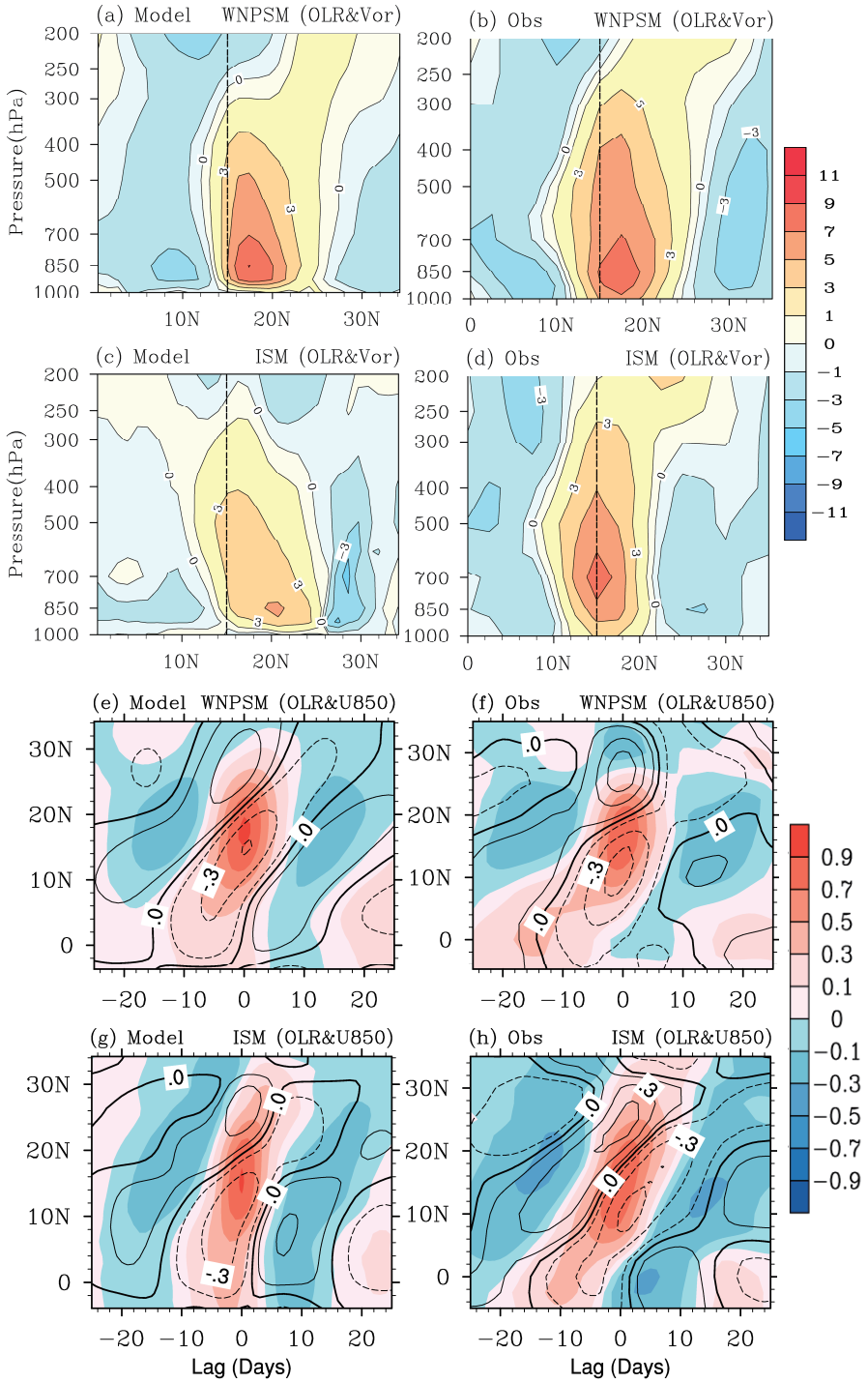

Fig. 4. (a–d) Meridional–vertical structure of intraseasonal vorticity (units: 10^{-6} s^{-1}) along 110°–140°E/60°–90°E for the WNPSM/ISM. (e–h) Latitude–lag correlations of intraseasonal OLR (10°–25°N, 110°–140°E)/(7.5°–22.5°N, 60°–90°E) with 850-hPa zonal wind (contours) and OLR (shaded) along 110°–140°E/60°–90°E for the WNPSM/ISM. Predictions by the model and observations are shown in the left and right columns, respectively. The dashed lines in (a–d) represent the position of the maximum convection center.

with the summer mean over the tropical western Pacific (Fig. 6b), which is attributed to their sensitivity to ENSO variability (Teng and Wang, 2003; Lin and Li, 2008). To a certain extent, the prediction captures this relationship, but with a more eastward range of significant correlation distributed over the tropical central Pacific (Fig. 6a).

The interannual correlations between seasonally averaged ISV anomaly (SAISV) and the JJAS mean of 850-hPa zonal wind are further shown in Figs. 6c and d. Observations present significant positive correlation over most of

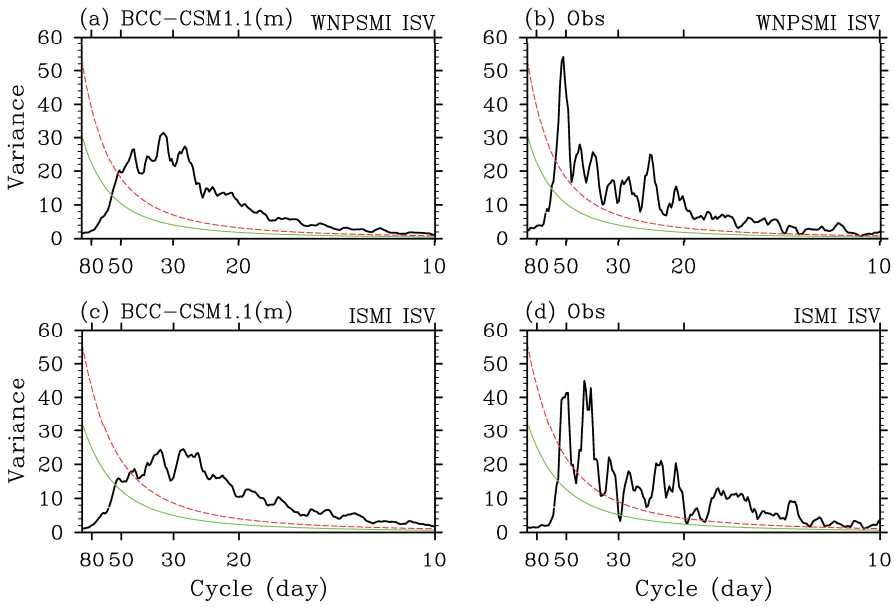

Fig. 5. Power spectra of the intraseasonal variability of (a, b) WNPSMI and (c, d) ISMI for model (left column) and observations (right column). The green and red lines denote red noise spectrums and 95% confidence bounds, respectively.

Asia and the western Pacific, especially the tropical western Pacific, where areas with correlation coefficients above 0.9 extend from the South China Sea to the east of the dateline (Fig. 6d). In contrast, relatively weaker correlation appears over the area from the tropical western South Indian Ocean across Somalia to the southern Arabian Sea and India (Fig. 6d), corresponding to an insignificant correlation between the SAISV and summer mean for the OLR over the Bay of Bengal and southern Indo-China Peninsula (figure not shown). This feature partially supports the result about the South Asian summer monsoon that the ISV anomaly itself may have little linear link with the summer mean (e.g., Qi et al., 2008; Achuthavarier and Krishnamurthy, 2010). The model, however, evidently overestimates the relationship between the SAISV and summer mean over the tropical central Pacific, and near Somalia and the southern Arabian Sea (Fig. 6c).

Table 1 further examines the interannual variation of the summer mean, intensity of ISV, and the SAISV for the WNPSMI and ISMI. Measured by the correlations between predictions and observations, prominent prediction skills are found only for the summer mean and SAISV of the WNPSMI with a correlation coefficient of about 0.7, but little skill for any of the other items of the WNPSMI and ISMI. Compared to observations, the model underestimates the connection between the summer mean and the intensity of ISV for both the WNPSMI and ISMI. Also, significant positive correlations between the summer mean and the SAISV are found for the above two dynamical monsoon indices in both prediction and observation, and a stronger-than-observed connection is especially captured by the model for the ISMI, as already partially revealed in Fig. 6.

A narrower-than-observed spectral band of ISV (Fig. 5) and an exaggerated relationship between the SAISV and summer mean of the ISM (Fig. 6 and Table 1) coexist in the model. To explore this feature, the frequencies of ISV anomalies in different monsoon years for the ISMI, as well as for the WNPSMI, are examined (Fig. 7). The strong, weak and normal monsoon years for a specific observed monsoon index are distinguished by a standardized anomaly of the JJAS mean index above 0.8, below −0.8, and between −0.8 and 0.8, respectively. According to these criteria, there are 5, 5, and 10 (4, 4, and 12) strong, weak and normal years for the observed WNPSMI (ISMI) from 1991 to 2010. Both the ensemble average and individual members of predictions show a similar proportion of frequency of certain

Table 1. Interannual correlations between predictions and observations for some relevant items of western North Pacific summer monsoon index (WNPSMI) and Indian summer monsoon index (ISMI), and correlations between two of the items for model and observations. Values in bold font exceed the confidence level of 99%.

	Model & Obs			ISV Std & JJAS mean		SAISV & JJAS mean	
	JJAS mean	ISV Std	SAISV	Model	Obs	Model	Obs
NPSMI	**0.69**	0.36	**0.71**	−0.06	0.33	**0.91**	**0.92**
ISMI	−0.17	0.30	0.27	0.09	0.33	**0.88**	**0.75**

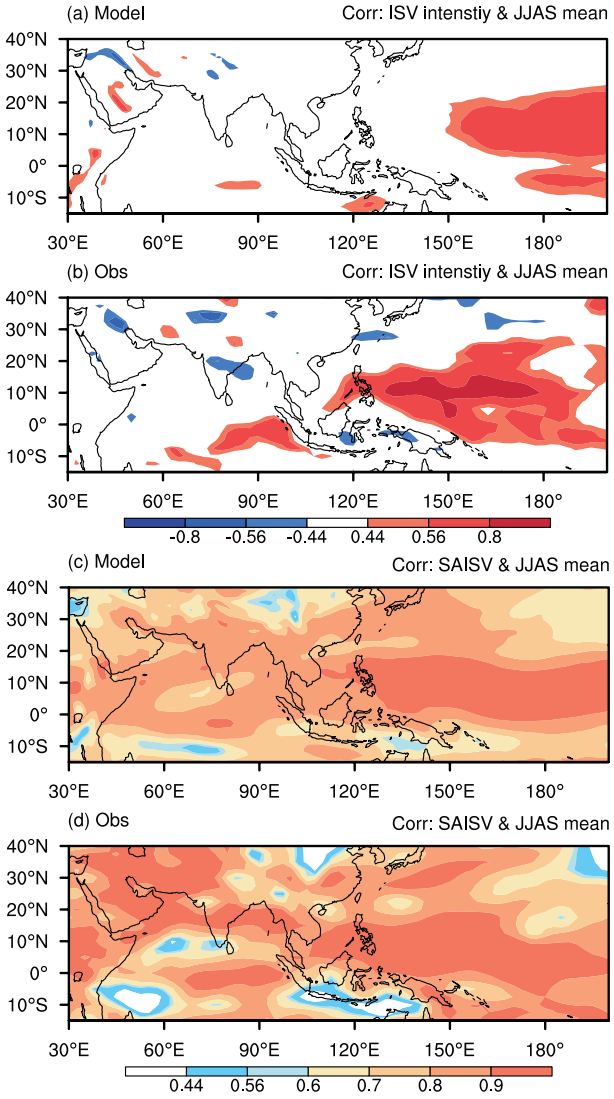

Fig. 6. Spatial distributions of temporal correlations between (a, b) the intensity of intraseasonal variability and summer mean and (c, d) the seasonal average of intraseasonal variability and summer mean from 1991 to 2010 for 850-hPa zonal wind in (a, c) the model and (b, d) observations.

monsoon years in general; however, only about 40%, 40% and 60% (25%, 25% and 67%) of strong, weak and normal WPNSM (ISM) years in observations are consistently captured by the model. Here, the statistics of ISV and IAV anomalies for each one of the 15 members are individually computed before showing the general ensemble features. Figure 7 indicates that, in both the model and observations, the phase of ISV is often characterized by a shift towards more frequent active (break) events in the strong (weak) summer monsoon years, and a smaller change in the normal monsoon years. This feature suggests that the frequency of active and break cycles of ISV is distinguishable between a strong and weak monsoon year, which supports the hypothesis that the IAV of seasonal mean monsoon may partially result from the shifts in the probability of the phase of the ISV (e.g., Palmer, 1994; Sperber et al., 2000; Goswami and Ajaya Mohan, 2001).

Although the model exhibits a reasonable prediction skill in the link between IAV and the frequency of ISV phases, it may not be necessary to support a reliable contribution of ISV to the summer mean monsoon. The very-long-duration active or break phases of ISV can act as a common seminal factor for generating anomalous seasons (Joseph et al., 2009; Krishnan et al., 2009; Joseph et al., 2010) and are rather important for the non-triviality of SAISV in a whole summer. Thus, the frequency of long break (active) spells and the strong/normal/weak monsoon years co-occurring with long break (active) spells are further explored in Table 2. The long break (active) spells here are identified as break (active) phases of ISV with consecutive standardized anomalies below -1.0 (above 1.0) and a duration of at least 10 days for the WNPSMI or ISMI. Statistics for the predictions are based on all ensemble members. As seen from columns b and d in Table 2, about 50% of the long break (active) spells occur in weak (strong) monsoon years and the sum of long break (active) spells during weak (strong) and normal monsoon years stands at around 90%, as indicated by both the model prediction and observations. Further, columns a and c in Table 2 show that a considerable proportion of normal and weak (strong) monsoon years is associated with long break (active) spells. For the more frequent occurrence and higher consistency between forecasts and observations for normal monsoon years compared to weak and strong monsoon years, the overestimated frequency of long breaks and underestimated frequency of long active spells in normal ISM years favor the non-triviality of SAISV in those years and further contribute to the summer mean, which may be part of the reason why a stronger-than-observed relationship between the SAISV and IAV of the ISM is captured by the model.

5. Link with external forcing and circulation

The links of the WNPSMI and ISMI on various forms [i.e., summer mean, SAISV, and seasonally averaged longwave variability (SALWV)] with summer mean SST, low-level winds and precipitation are further explored.

The correlations between JJAS mean SST and the summer mean, SAISV, and SALWV of the WNPSMI for the model and observations are given in Figs. 8a–f. Also, the connections between the WNPSMI of different forms and JJAS mean circulation are shown in Figs. 9a–f. It is observed that a stronger-than-normal summer mean WNPSMI is associated with a positive SST anomaly over the equatorial central Pacific and a negative SST anomaly over the northeast of Australia, eastern Indonesian Islands, and region from the eastern Bay of Bengal to the Philippine Sea (Fig. 8b). It not only corresponds to a belt of westerly wind anomaly across the Maritime Continent and the tropical western Pacific surrounded by anomalies of cyclonic wind convergence over its both sides in the two hemispheres, but also is coupled with more precipitation over the tropical western Pacific and less precipitation over a cross-equatorial sloping belt from Aus-

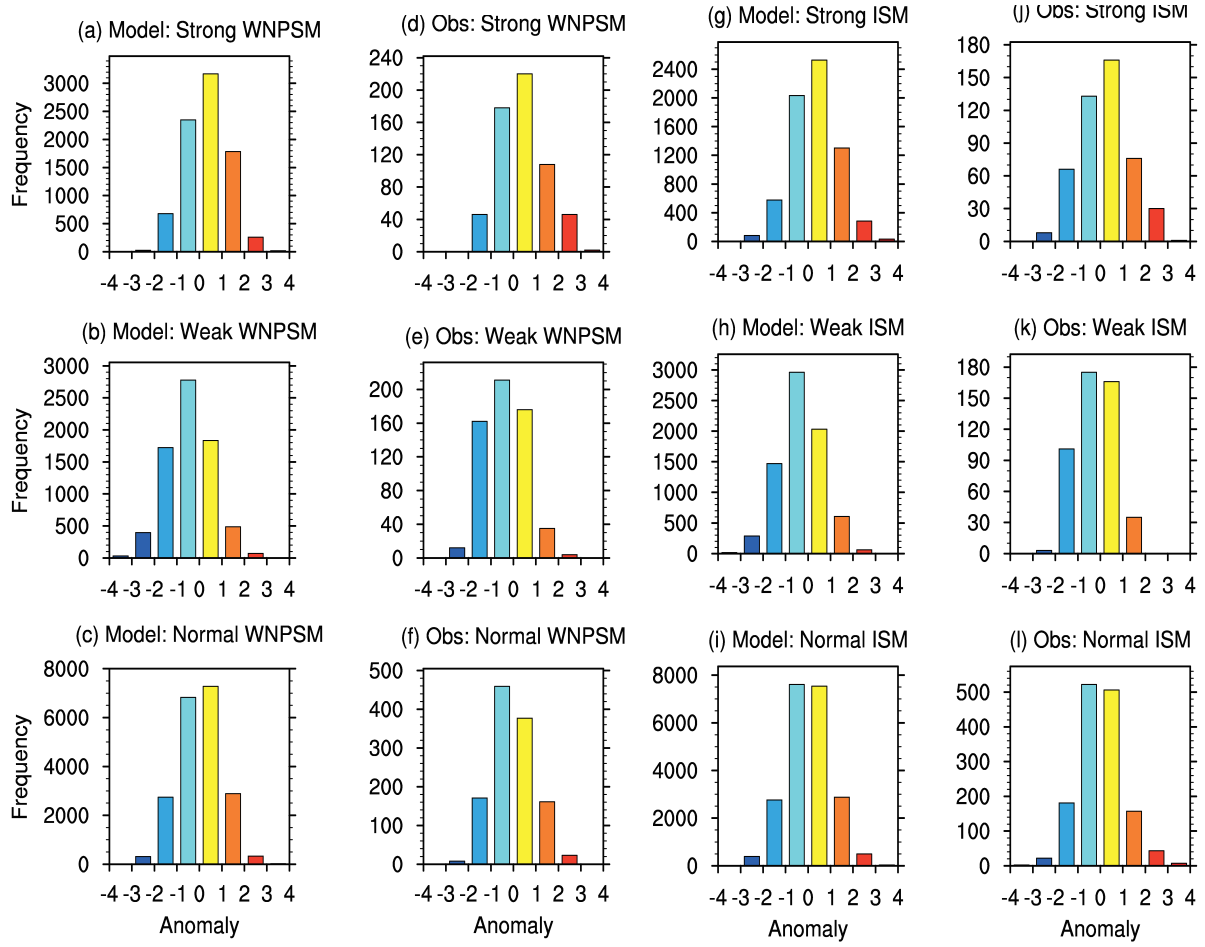

Fig. 7. Frequencies of intraseasonal anomalies of (a–f) WNPSMI and (g–l) ISMI in strong (upper row), weak (middle row) and normal (bottom row) monsoon years for (a–c; g–i) the model and (d–f; j–l) observations.

Table 2. The frequencies (units: %) of long break/active spells (LBS/LAS) and anomalous summer monsoon years co-occurring with LBS/LAS. Monsoon years are classified into weak, normal and strong ones according to the magnitude of standardized anomalies of the summer-mean WNPSMI and ISMI.

	(a) Certain monsoon years with LBS/sum of these monsoon years		(b) LBS occurring in certain monsoon years/sum of LBS		(c) Certain monsoon years with LAS/sum of these monsoon years		(d) LAS occurring in certain monsoon years/sum of LAS	
	Model	Obs	Model	Obs	Model	Obs	Model	Obs
Weak WNPSM	85.2	60.0	57.5	50.0	8.2	20.0	3.9	9.1
Normal WNPSM	30.0	40.0	39.7	50.0	30.6	40.0	50.0	45.5
Strong WNPSM	5.8	0.0	2.8	0.0	59.4	60.0	46.1	45.4
Weak SASM	59.7	50.0	53.1	57.1	4.8	0.0	5.5	0.0
Normal SASM	21.5	16.7	42.7	28.6	19.9	33.3	54.2	57.1
Strong SASM	7.0	25.0	4.2	14.3	42.1	75	40.3	42.9

tralia across Indonesia to India (Fig. 9b). Similar to the findings by Wang et al. (2000), the above features may be supported by air–sea interaction processes, in which the strengthening westerly wind (weakening easterly trade) over the east (west) of the Philippine Sea encourages the cooling (warming) SST by enhanced (suppressed) evaporation and entrainment cooling over respective regions. The distribution of SST anomalies over the tropical western Pacific in turn favors the persistence of wind anomalies through an atmospheric thermal response. Although sharing a similar correlation pattern as above, the SAISV and SALWV of the WNPSMI are correlated with SST with different priorities, in which the former is related more to the SST over the region from the Bay of Bengal to the Philippine Sea and less to the SST over the equatorial central Pacific, while the latter often shows a very similar connection with SST to that of the summer-mean WNPSMI

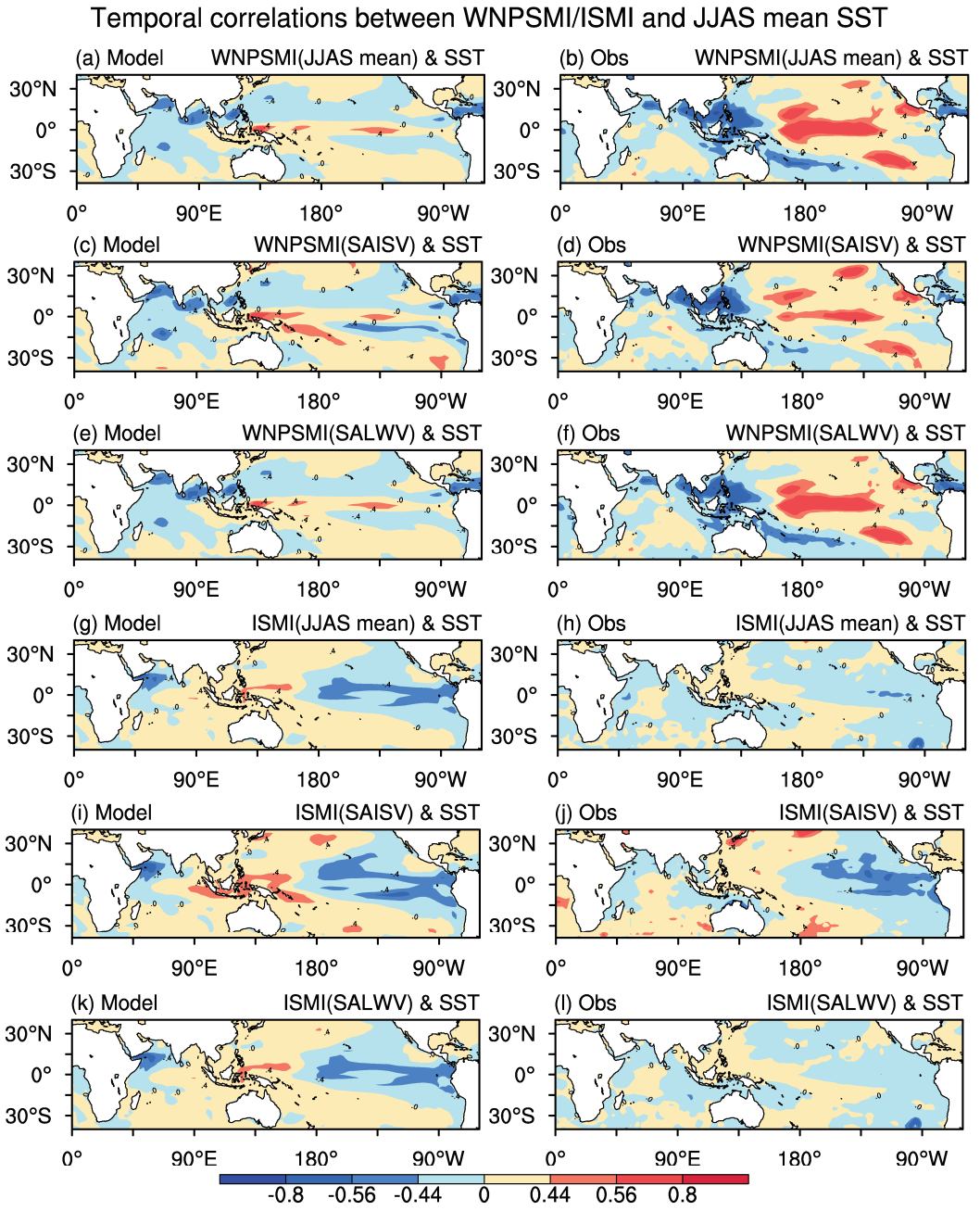

Fig. 8. Patterns of correlations between summer-mean SST and WNPSMI/ISMI for the model (left column) and observations (right column). The monsoon index is examined by the summer mean (a, b; g, h), seasonal average of intraseasonal variability (c, d; i, j), and seasonal average of long-wave variability (e, f; k, l), respectively. The shading levels above 0.44 and 0.56 (below −0.44 and −0.56) represent the statistical significance of correlation above the 95% and 99% confidence levels, respectively.

(Figs. 8d, f). In association, a significant response feature of low-level winds is confined to the west of the dateline for the SAISV, while it extends into the tropical central Pacific for the SALWV (Figs. 9d and f).

The summer-mean WNPSMI in the model almost shows no significant connections with SST except over some very small and sparse regions in the tropical Indian Ocean and western Pacific (Fig. 8a). Meanwhile, a regional cyclonic wind response over the western Pacific is captured by the model (Fig. 9a). These features are almost equivalently reproduced by the results for the SAISV and SALWV of the WNPSMI, indicating that the seasonal contributions of monsoon variability with different scales tend to show a common link with external forcing and circulation rather than a selective connection (Figs. 8c, e, 9c and e).

The links of predicted and observed summer mean, SAISV and SALWV of the ISMI with JJAS mean SST are presented in Figs. 8g–l, and with JJAS mean 850-hPa winds

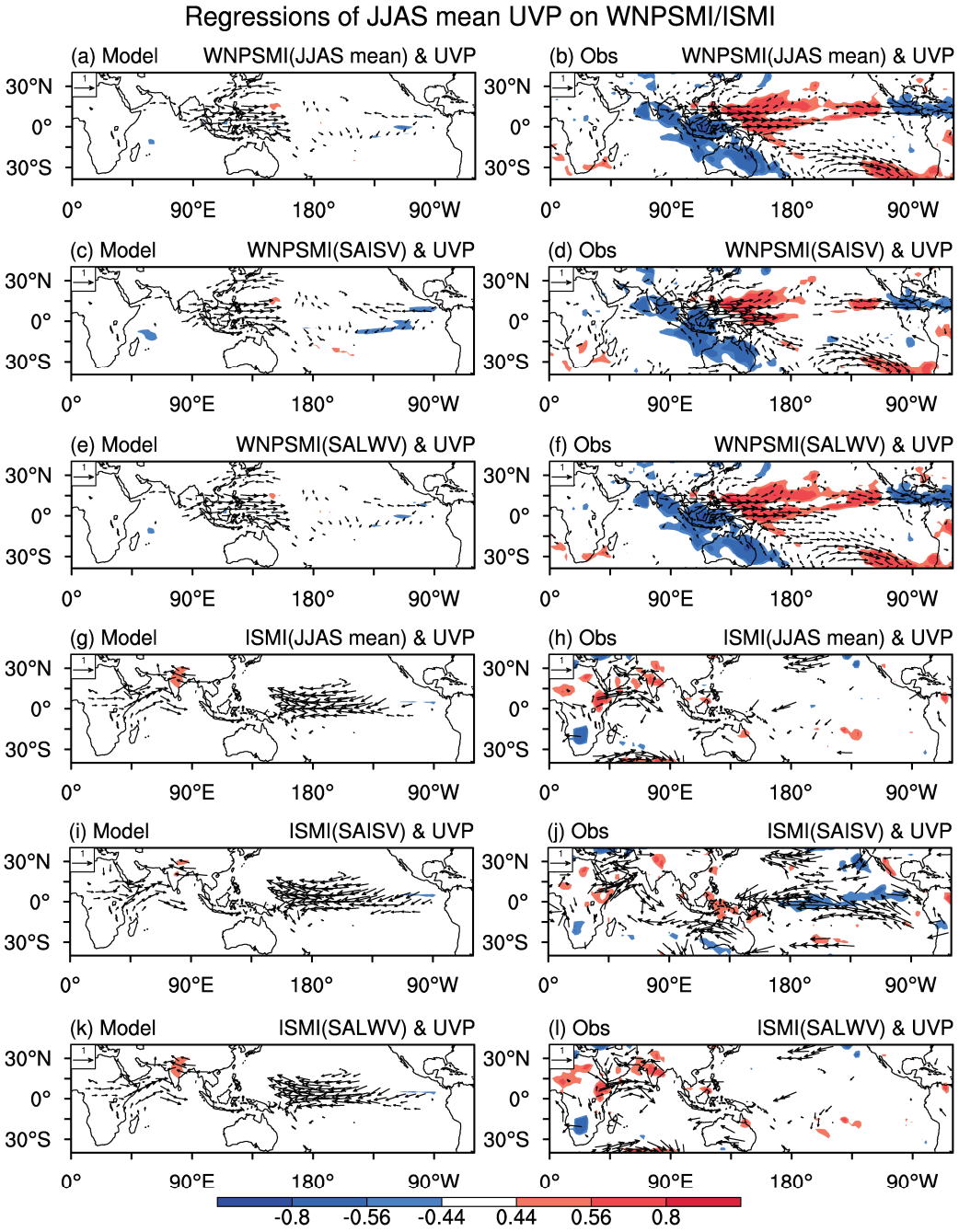

Fig. 9. Patterns of regressions (vectors) of summer-mean 850-hPa winds on WNPSMI/ISMI and correlations (shading) between summer-mean precipitation and WNPSMI/ISMI for the model (left column) and observations (right column). The monsoon index is examined by the summer mean (a, b; g, h), seasonal average of intraseasonal variability (c, d; i, j), and seasonal average of long-wave variability (e, f; k, l), respectively. The shading and vectors represent the statistical significance of correlation above the 95% confidence level.

and precipitation in Figs. 9g–l. The summer mean of ISMI shows a negative but insignificant correlation with the SST over the tropical central and eastern Pacific and the tropical western North Indian Ocean (Fig. 8h), in association with a significant correlation with zonal wind over most of the Arabian Sea (Fig. 9h). These observational features essentially indicate a degree of teleconnection between ENSO and ISM, although overtaken by an obvious decline since the 1980s in contrast to before that time (e.g., Kumar et al., 1999; Wang et al., 2001; Kripalani et al., 2003). Similar to the results for the WNPSMI, the SAISV and SALWV of the ISMI are also correlated with SST with similar patterns but different details. In particular, over the tropical eastern Pacific, the SAISV is more apparently and negatively correlated with SST and low-

level zonal wind than the SALWV and summer mean (Figs. 8j and 9j), implying a strong link between ENSO and the ISV of the ISM.

For the ISM in the model, however, the summer mean, SAISV and SALWV are all significantly related to SST and circulation over the tropical central and eastern Pacific and the differences among them are small (Figs. 8g, i, k, 9g, i, and k). Additionally, the negative correlations with SST in the tropical eastern Pacific and western Indian Ocean, as well as the horseshoe patterns of positive correlation in the western Pacific and part of the tropical eastern Indian Ocean are similar to the La Niña SST anomaly distribution. To some extent, these features indicate an overestimation of the link between the ISM and ENSO.

Given the critical role of ENSO in seasonal climate forecasts, we assess the prediction skills for ENSO and its impact on monsoon circulation. If the interannual departures of Niño3.4 SST above 0.5°C or below −0.5°C in each month from March to September in the 20 years are chosen as significant anomalies of ENSO, 64 and 68 anomalous months are observed and predicted, respectively, and 41 of them are consistently captured by both the model and observations. The correlation between prediction and observation in all forecast months is 0.78, suggesting a reasonable skill for ENSO forecasting. However, the observed connections between monsoon and SST in the Niño region are limitedly reproduced by the model as presented in Figs. 8 and 9. Due to the small differences among the multiscale responses of monsoon to tropical SST and circulation in the model, we further examine the impact of ENSO on seasonal mean circulation. Figures 10a–d show the simultaneous relationships between the Niño3.4 SST index and the 850-hPa winds and precipitation for both predictions and observations in summer and spring. Also, the correlations between the Niño3.4 SST index and tropical SST are shown in Figs. 10e–h. In summer, when ENSO is in a developing or decaying stage, significant large-scale atmospheric responses are mainly observed over the subtropical South Pacific and the tropical region from the eastern Indian Ocean to the eastern Pacific (Fig. 10b), associated with an in-phase SST anomaly over the eastern Pacific and a horseshoe-pattern response over the western Pacific (Fig. 10f). However, the model evidently underestimates the responses of winds and precipitation over most of the tropical Pacific and the tropical eastern Indian Ocean (Fig. 10a), in association with narrower-than-observed significant correlation of SST over the central-eastern Pacific (Fig. 10e). Compared to that in summer, the model basically reproduces the connections between the Niño3.4 index and tropical SST and circulation in spring (Figs. 10c, d, g, and h). Therefore, the too-rapid decrease in the impact of ENSO with forecast time should be partially responsible for the apparent underestimation of the relationship of the WNPSM with SST and circulation.

6. Summary and discussion

In this study, we have explored the relationship between the IAV and ISV of the Asian–western Pacific monsoon using retrospective forecasts initialized at the end of February by the BCC_CSM1.1(m).

The model exhibits reasonable skill in its predictions of climatologies and the IAV of monsoon, in spite of some apparent systematic biases, and it performs better with respect to the IAV of the WNPSM than that of the ISM. In terms of the standard deviations of the ISV and IAV of summer monsoon, the model also reasonably reproduces the observed features of spatial distribution, but with larger amplitude and a farther eastward position of the central strength for both. Besides, narrower-than-observed spectral bands for the WNPSM and ISM on the intraseasonal scale are found in the model since the predicted spectral variances are mainly limited to the bands with periods of less than 50 days.

The model shows positive interannual correlation between the summer mean and intensity of ISV over the western Pacific, but with a more eastward shift of significant correlation compared to observation. Also, the predictions show a stronger-than-observed connection between the summer mean and SAISV over the tropical central Pacific and near Somalia and the southern Arabian Sea. The statistics on the frequencies of ISV anomalies in strong, weak, and normal WNPSM and ISM years indicate that the seasonal anomalies of summer monsoon are to a certain extent determined by the shifts in probability of ISV towards either an active or break phase. Although the model can basically reproduce this feature, it still overestimates the frequency of long breaks and underestimates the frequency of long active spells in normal Indian monsoon years, which may partially contribute to the stronger-than-observed relationship between the SAISV and seasonal mean of the ISM.

Furthermore, the interannual links of the seasonal mean, SAISV and SALWV of the WNPSMI and ISMI with summer mean SST, low-level winds and precipitation have been explored. Observations reveal that, the seasonal mean, SAISV and SALWV of summer monsoon all show similar correlation patterns with summer SST but with different details. For the WNPSMI, both seasonal mean and SALWV are significantly and positively correlated with SST over the equatorial central Pacific but negatively correlated with SST over the northeast of Australia, eastern Indonesian Islands, and regions from the eastern Bay of Bengal to the Philippine Sea. The correlation between SAISV and SST is concentrated more in the region from the Bay of Bengal to the Philippine Sea and less in the equatorial central Pacific. However, the predicted seasonal mean, SAISV, and SALWV of the WNPSMI present highly similar links with SST, and the correlations are insignificant except over some small and sparse regions in the tropical Indian Ocean and the western Pacific. It is supposed that the excessive decline of the impact of ENSO with forecast time should partially account for the apparent underestimation of the relationship of the WNPSM with SST and circulation. For the ISMI, the observed seasonal mean and SALWV show similar but insignificant correlations with the SST over most tropical areas, while significant correlation between SAISV and tropical eastern Pacific SST is found. Nevertheless, not only stronger-than-observed

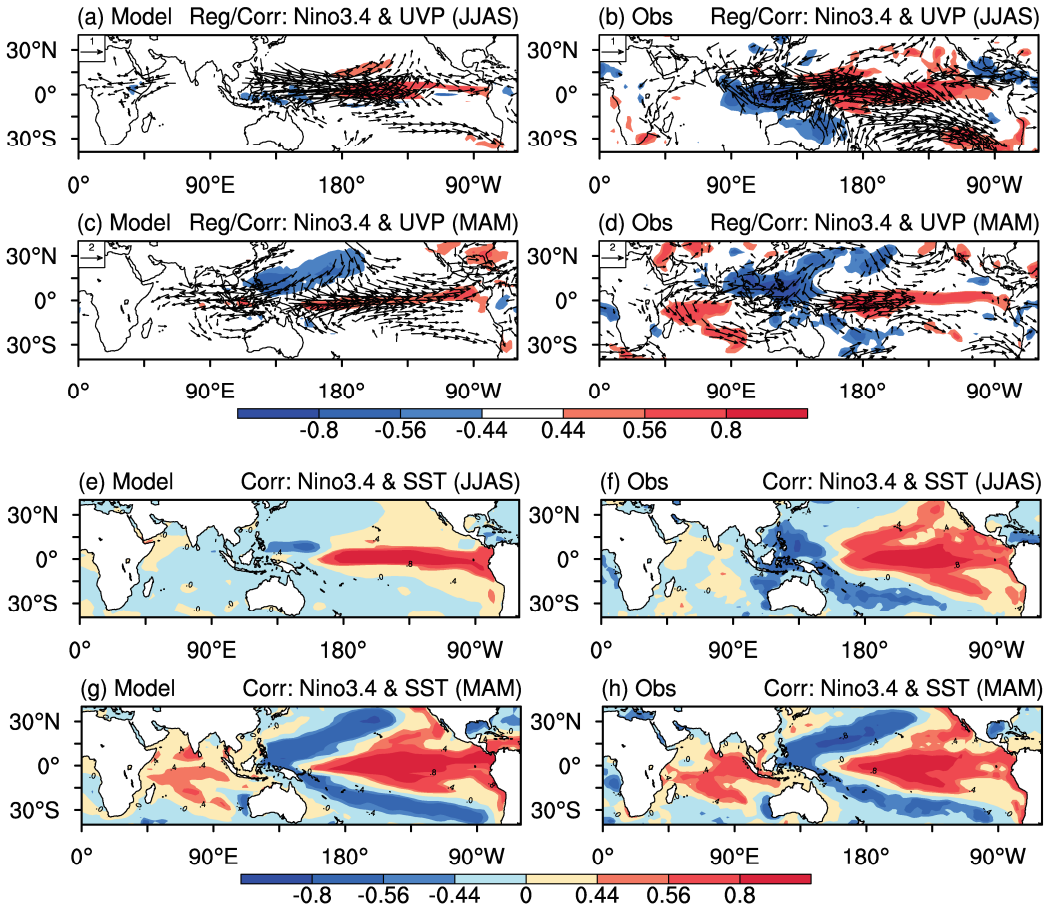

Fig. 10. (a–d) Patterns of regressions (vectors) of seasonal mean 850-hPa winds on Niño3.4 SST index and correlations (shading) between precipitation and Niño3.4 SST index for the (a, c) model and (b, d) observations. The features for the summer (June to September) and spring (March to May) are given in (a, b) and (c, d), respectively. Panels (e–h) are the same as (a–d), but only for the correlations between SST and Niño3.4 index.

relationships with SST over the tropical eastern Pacific, but also very small differences among these correlation distributions for the seasonal mean, SAISV and SALWV of the ISMI are captured by the model, implying an overestimated link between the ISM and ENSO. The features of low-level circulation and precipitation also match the above results.

The BCC_CSM1.1(m) shows reasonable but limited skill in capturing the observed relationships between the ISV and IAV of summer monsoon. However, this may gradually improve with a decrease in the lead time of prediction given that the current hindcasts initialized at the end of February most likely suffer from a spring predictability barrier. Thus, more experiments and evaluations on this subject should be implemented in future work. Meanwhile, our analyses have revealed some shortcomings of the model in forecasting the relationships between the ISV and IAV of monsoon and have preliminarily explored the possible causes, suggesting that we should pay attention to further improving the model's ability in capturing ENSO events and their links with atmospheric circulation, as well as in reproducing monsoon ISV with accurate spectral characteristics and reasonable frequencies of long breaks or active spells.

In addition, it should be noted that the ensemble prediction of the WNPSM exhibits more skill than that of the ISM, as demonstrated in section 3, which is also found in predictions of the Asian summer monsoon by the NCEP Climate Forecast System (e.g., Jiang et al., 2013). Two factors may account for this feature. First, compared to the ISM, the WNPSM is more highly correlated with ENSO and large-scale circulation on the interannual scale (e.g., Wang et al., 2000; Xie et al., 2009), which can be relatively better captured by the ensemble prediction of models. Secondly, the interannual variability of the ISM is affected not only by ENSO, but also by local SST (e.g., the Indian Ocean dipole) and thermal conditions over the surrounding lands such as the Tibetan Plateau, leading to more complex and less skillful prediction of the ISM. Further studies on this issue are undoubtedly necessary.

Acknowledgements. The authors thank the three anonymous reviewers for their constructive comments, which improved the overall quality of this paper. This study was partially supported by the National Natural Science Foundation of China (Grant Nos. 41305057, 41275076, 41105069, and 41375081), the National Ba-

sic Research Program of China (Grant Nos. 2010CB951903 and 2014CB953900) and the LCS Youth Fund (2014).

REFERENCES

Achuthavarier, D., and V. Krishnamurthy, 2010: Relation between intraseasonal and interannual variability of the South Asian monsoon in the national Centers for Environmental Predictions forecast systems. *J. Geophys. Res.*, **115**, D08104, doi: 10.1029/2009JD012865.

Charney, J. G., and J. Shukla, 1981: Predictability of monsoons. *Monsoon Dynamics*, J. Lighthill and R. P. Pearce, Eds., Cambridge University Press, Cambridge, 99–109.

Drbohlav, H., and V. Krishnamurthy, 2010: Spatial structure, forecast errors, and predictability of the South Asian monsoon in CFS monthly retrospective forecasts. *J. Climate*, **23**, 4750–4769.

Ferranti, L., J. M. Slingo, T. N. Palmer, and B. J. Hoskins, 1997: Relations between interannual and intraseasonal monsoon variability as diagnosed from AMIP integrations. *Quart. J. Roy. Meteor. Soc.*, **123**, 1323–1357.

Fujinami, H., and Coauthors, 2011: Characteristic intraseasonal oscillation of rainfall and its effect on interannual variability over Bangladesh during boreal summer. *Int. J. Climatol.*, **31**, 1192–1204.

Goswami, B. N., 1998: Interannual variation of Indian summer monsoon in a GCM: External conditions versus internal feedbacks. *J. Climate*, **11**, 501–522.

Goswami, B. N., and R. S. Ajaya Mohan, 2001: Intraseasonal oscillations and interannual variability of the Indian summer monsoon. *J. Climate*, **14**, 1180–1198.

Goswami, B. N., and P. K. Xavier, 2005: Dynamics of "internal" interannual variability of the Indian Summer Monsoon in a GCM. *J. Geophys. Res.*, **110**, D24104, doi: 10.1029/2005JD006042.

Goswami, B. N., G. Wu, and T. Yasunari, 2006: The annual cycle, intraseasonal oscillations, and roadblock to seasonal predictability of the Asian summer monsoon. *J. Climate*, **19**, 5078–5099.

Jiang, X., S. Yang, Y. Li, A. Kumar, X. Liu, Z. Zuo, and B. Jha, 2013: Seasonal-to-interannual prediction of the Asian summer monsoon in the NCEP Climate Forecast System Version 2. *J. Climate*, **26**, 3708–3727.

Joseph, S., A. K. Sahai, and B. N. Goswami, 2009: Eastward propagating MJO during boreal summer and Indian monsoon droughts. *Climate Dyn.*, **32**, 1139–1153.

Joseph, S., A. K. Sahai, and B. N. Goswami, 2010: Boreal summer intraseasonal oscillations and seasonal Indian monsoon prediction in DEMETER coupled models. *Climate Dyn.*, **35**, 651–667.

Kanamitsu, M., W. Ebisuzaki, J. Woollen, S. K. Yang, J. J. Hnilo, M. Fiorino, and G. L. Potter, 2002: NCEP-DEO AMIP-II Reanalysis (R-2). *Bull. Amer. Meteor. Soc.*, **83**, 1631–1643.

Kang, I. S., and J. Shukla, 2006: Dynamic seasonal prediction and predictability of the monsoon. *The Asian Monsoon*, Springer, 585–612.

Kim, H. M., I. S. Kang, B. Wang, and J. Y. Lee, 2008: Interannual variations of the boreal summer intraseasonal variability predicted by ten atmosphere-ocean coupled models. *Climate Dyn.*, **30**, 485–496.

Kripalani, R. H., A. Kulkarni, S. S. Sabade, and M. L. Khandekar, 2003: Indian monsoon variability in a global warming scenario. *Nat. Hazards*, **29**, 189–206.

Krishnamurthy, V., and J. Shukla, 2000: Intraseasonal and interannual variability of rainfall over India. *J. Climate*, **13**, 4366–4377.

Krishnamurthy, V., and J. Shukla, 2007: Intraseasonal and seasonally persisting patterns of Indian monsoon rainfall. *J. Climate*, **20**, 3–20.

Krishnamurthy, V., and J. Shukla, 2008: Seasonal persistence and propagation of intraseasonal patterns over the Indian monsoon region. *Climate Dyn.*, **30**, 353–369.

Krishnan, R., V. Kumar, M. Sugi, and J. Yoshimura, 2009: Internal feedbacks from monsoon–midlatitude interactions during droughts in the Indian summer monsoon. *J. Atmos. Sci.*, **66**, 553–578.

Kumar, K. K., B. Rajagopalan, and M. A. Cane, 1999: On the weakening relationship between the Indian monsoon and ENSO. *Science*, **284**, 2156–2159.

Lawrence, D. M., and P. J. Webster, 2001: Interannual variations of the intraseasonal oscillation in the South Asian summer monsoon region. *J. Climate*, **14**, 2910–2922.

Lee, J. Y., and Coauthors, 2010: How are seasonal prediction skills related to models' performance on mean state and annual cycle? *Climate Dyn.*, **35**, 267–283.

Li, C., R. Lu, and B. Dong, 2012: Predictability of the western North Pacific summer climate demonstrated by the coupled models of ENSEMBLES. *Climate Dyn.*, **39**, 329–346.

Liebmann, B., and C. A. Smith, 1996: Description of a complete (interpolated) outgoing longwave radiation dataset. *Bull. Amer. Meteor. Soc.*, **77**, 1275–1277.

Lin, A., and T. Li, 2008: Energy spectrum characteristics of boreal summer intraseasonal oscillations: climatology and variations during the ENSO developing and decaying phases. *J. Climate*, **21**, 6304–6320.

Liu, X. W., S. Yang, A. Kumar, S. Weaver, and X. W. Jiang, 2013: Diagnostics of subseasonal prediction biases of the Asian summer monsoon by the NCEP Climate Forecast System. *Climate Dyn.*, **41**, 1453–1474, doi: 10.1007/s00382-012-1553-3.

Liu, X. W., S. Yang, Q. P. Li, A. Kumar, S. Weaver, and S. Liu, 2014: Subseasonal forecast skills and biases of global summer monsoons in the NCEP Climate Forecast System version 2. *Climate Dyn.*, **42**, 1487–1508, doi: 10.1007/s00382-013-1831-8.

Palmer, T. N., 1994: Chaos and predictability in forecasting the monsoons. *Proc. Indian Natl. Sci. Acad.*, **60A**, 57–66.

Qi, Y. J., R. H. Zhang, T. Li, and M. Wen, 2008: Interactions between the summer mean monsoon and the intraseasonal oscillation in the Indian monsoon region. *Geophys. Res. Lett.*, **35**, L17704, doi: 10.1029/2008GL034517.

Rajeevan, M., C. K. Unnikrishnan, and B. Preethi, 2012: Evaluation of the ENSEMBLES multi-model seasonal forecasts of Indian summer monsoon variability. *Climate Dyn.*, **38**, 2257–2274.

Reynolds, R. W., N. A. Rayner, T. M. Smith, D. C. Stokes, and W. Wang, 2002: An improved in situ and satellite SST analysis for climate. *J. Climate*, **15**, 1609–1625.

Sperber, K. R., J. M. Slingo, and H. Annamalai, 2000: Predictability and relationship between subseasonal and interannual variability during the Asian summer monsoon. *Quart. J. Roy. Meteor. Soc.*, **126**, 2545–2574.

Suhas, E., J. M. Neena, and B. N. Goswami, 2012: Interannual

variability of Indian summer monsoon arising from interactions between seasonal mean and intraseasonal oscillations. *J. Atmos. Sci.*, **69**, 1761–1774.

Teng, H., and B. Wang, 2003: Interannual variations of the boreal summer intraseasonal oscillation in the Asian-Pacific region. *J. Climate*, **16**, 3572–3584.

Waliser, D. E., R. Murtugudde, and L. E. Lucas, 2004: Indo-Pacific Ocean response to atmospheric intraseasonal variability. Part II: boreal summer and the intraseasonal oscillation. *J. Geophys. Res.*, **109**, C03030, doi: 10.1029/2003JC002002.

Wang, B., R. Wu, and X. Fu, 2000: Pacific-East Asia teleconnection: How does ENSO affect East Asian climate? *J. Climate*, **13**, 1517–1536.

Wang, B., R. Wu, and K. M. Lau, 2001: Interannual variability of Asian summer monsoon: Contrast between the Indian and western North Pacific-East Asian monsoons. *J. Climate*, **14**, 4073–4090.

Wang, B., and Coauthors, 2008: How accurately do coupled climate models predict the leading modes of Asian–Australian monsoon interannual variability? *Climate Dyn.*, **30**, 605–619.

Wu, T., and Coauthors, 2010: The Beijing Climate Center atmospheric general circulation model: Description and its performance for the present-day climate. *Climate Dyn.*, **34**, 123–147.

Wu, T. W., and Coauthors, 2013: Global carbon budgets simulated by the Beijing Climate Center climate system model for the last century. *J. Geophys. Res.*, **118**, 1–22, doi: 10.1002/jgrd.50320.

Xavier, P. K., J. P. Duvel, and J. D. Francisco, 2008: Boreal summer intraseasonal variability in coupled seasonal hindcasts. *J. Climate*, **21**, 4477–4497.

Xie, P., and P. A. Arkin, 1997: Global precipitation: A 17-year monthly analysis based on gauge observations, satellite estimates, and numerical model outputs. *Bull. Amer. Meteor. Soc.*, **78**, 2539–2558.

Xie, S., K. Hu, J. Hafner, H. Tokinaga, Y. Du, G. Huang, and T. Sampe, 2009: Indian Ocean capacitor effect on Indo-western Pacific climate during the summer following El Niño. *J. Climate*, **22**, 730–747.

Xie, S., H. Ma, J. Boyle, S. Klein, and Y. Zhang, 2012: On the correspondence between short- and long-time-scale systematic errors in CAM4/CAM5 for the year of tropical convection. *J. Climate*, **25**, 7937–7955.

Xue, Y., and Coauthors, 2010: Intercomparison and analyses of the climatology of the West African monsoon in the West African monsoon modeling and evaluation project (WAMME) first model intercomparison experiment. *Climate Dyn.*, **35**, 3–27.

Yang, S., Z. Zhang, V. Kousky, R. W. Higgins, S. H. Yoo, J. Liang, and Y. Fan, 2008: Simulations and seasonal prediction of the Asian summer monsoon in the NCEP Climate Forecast System. *J. Climate*, **21**, 3755–3775.

Yoo, J. H., W. R. Andrew, and I. S. Kang, 2010: Analysis of intraseasonal and interannual variability of the Asian summer monsoon using a hidden Markov model. *J. Climate*, **23**, 5498–5516.

Zhou, T., B. Wu, and B. Wang, 2009: How well do atmospheric general circulation models capture the leading modes of the interannual variability of the Asian–Australian monsoon? *J. Climate*, **22**, 1159–1173.